An improved equation for crystal size distribution in second-phase influenced aggregates

ALFONS BERGER*

Institute of Geological Sciences, University of Bern, Baltzerstrasse 1, CH-3012 Bern, Switzerland

ABSTRACT

A model is presented to calculate crystal size distributions (CSDs) for coarsened mineral aggregates. The equations consider the second-phase particles inside coarsening aggregates. This approach is different from other published kinetic growth equations. The proposed model includes grain size limits due to the presence of second-phase particles. These limits control the behavior of growing grains. The physical basis for this model is taken from a neighborhood-coarsening model. The model is able to compute coarsening of a given set of crystal sizes, to simulate the evolution of the CSD, and to describe the influence of the amount and size of the second-phase particles. The model is limited to rocks that can be described as matrix with second phases. For very low second-phase concentrations (volume fraction <0.01), the model gives results similar to Lifshitz-Slyozov-Wagner models (LSW). In the case where the second-phase content is extremely high (volume fraction >0.5), the model would not allow coarsening or the system can be no longer described as matrix and second-phase particles. Depending on the size and amount of second phases, the CSD develops similar to LSW at high growth rates, but intermediate growth rates produce CSDs that are unknown in other closed-system coarsening models.

To test the model, natural data from a contact-metamorphic calcite marble with different mica contents have been compared with simulated CSDs. The measured and simulated CSDs can be well described by the proposed model for variable amounts of second-phase particles. The two-phase model is applicable to impure carbonates, mica-bearing quartzites, or impure dunites. The proposed model has interesting applications to experimental data, where porosity may influence grain coarsening.

INTRODUCTION

Grain growth and recrystallization are key phenomena in understanding textures of rocks (e.g., Kretz 1994; Evans et al. 2001). The final grain size is a controlling parameter on deformation mechanisms, diffusion kinetics, and transport properties of rocks. In order to understand the physics of grain growth, experiments have been performed mainly on single-phase aggregates (e.g., Chai 1974; Nichols and Mackwell 1991; Masuda et al. 1997). However, several problems still hinder the extrapolation of these experimental data to natural, multiphase rocks (e.g., Covey-Crump 1997; Herwegh and Berger 2003). In particular, the use of experimental growth constants in natural examples requires information on the mechanisms of grain coarsening. Some of this necessary information is reflected by the crystal size distribution (CSD), and CSD analysis has proven fruitful in investigating textures and textural evolution in different rock types (e.g., Marsh 1998; Denison et al. 1997; Eberl et al. 2002; Higgins 2002). Theoretical models that allow an interpretation of a CSD have been developed mainly for nucleating and growing systems (e.g., Marsh 1988). However, it is well known that Ostwald ripening or other coarsening processes strongly influence the CSD (Higgins 1998; Cabane et al. 2001). In order to use CSD data in coarsened systems, grain growth is commonly modeled using the LSW theory (Lifshitz and Slyozov 1961; Wagner 1961). This theory offers equations for matrix-volume diffusion-controlled

coarsening, for matrix-grain-boundary-controlled diffusion and for dissolution/precipitation kinetics (Joesten 1991). In general, the LSW theory can be written as:

$$\frac{dR}{dt} = K_{(LSW)}\left(\frac{1}{R}\right)\left(\frac{1}{R^*} - \frac{1}{R}\right) \qquad (1)$$

where R^* is the critical radius, R is the grain radius, t is the time, and K is an empirical constant. Equation 1 has an analytical solution for pure grain growth and allows a stable CSD to be predicted for a certain amount of coarsening (Fig. 1).

A more general theory, called communication neighbor theory (CN) was presented by DeHoff (1991), which gives a solution for more complex microstructures and can be applied to polyphase aggregates. The CN theory considers the average distance between the coarsening grains such that Equation 1 changes to:

$$\frac{dR}{dt} = K\left(\frac{1}{\lambda}\right)\left(\frac{1}{R^*} - \frac{1}{R}\right) \qquad (2)$$

where $\langle 1/\lambda \rangle$ is the harmonic mean of the intercrystal distance. Growth does not depend on the length scale of the particle itself, but on the distance to the neighboring particle.

LSW and CN theory predict a CSD with a shift of the mode toward larger grain size and development of skewness toward the right-hand side (Fig. 1). Eberl et al. (1998) used the law of proportionate effects (LPE) to expand the crystal growth theory to encompass kinetic aspects. A simulation program (GALOPER) is available, in which closed-system coarsening
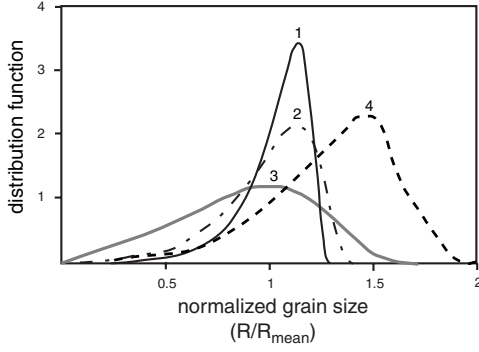
*E-mail: berger@geo.unibe.ch

FIGURE 1. Analytic solutions for different kinetic coarsening theories. Crystal size distribution functions are related to normalized grain size (R/R_{mean}) using LSW and CN theory (Lifshitz and Slyozov 1961; Wagner 1961; Joesten 1991; DeHoff 1991): (1) matrix volume diffusion; (2) matrix grain boundary diffusion; (3) particle/matrix interface reaction kinetics; and (4) CN theory. Graphs 1–3 were calculated on the basis of Equations 28–31 in Joesten (1991). Graph 4 is from deHoff (1991).

can be combined with nucleation and growth laws of different types (Eberl et al. 2000).

The final CSD is influenced by different physical processes (e.g., Marsh 1998; Higgins 1998, 2002; Eberl et al. 1998). However, in a completely crystalline starting material, we can assume grain coarsening as a closed-system process, where individual grains grow at the expense of smaller grains by moving grain boundaries (e.g., Chai 1974; Brook 1976; Kretz 1994; Evans et al. 2001). Such coarsening is fundamental in metamorphic rocks (Kretz 1994) and is also considered important in magmatic systems (e.g., Higgins 2002). The well-established kinetic theories assume diffusional processes or local dissolution and reprecipitation between neighboring grains, but ignore the influence of the non-growing solid material in the aggregates. In the following, I will also consider this material, which is usually referred as "second-phase particles" (Nes et al. 1985; Evans et al. 2001).

I propose a model in which the effect of second-phase particles is included into a general coarsening equation. This model is of special importance in geological materials, which are rarely pure single-phase aggregates. Certain kinds of metamorphic rocks (e.g., quartzites, carbonates, dunites) and porosity during low-grade metamorphism or in experiments, can be well described as matrix mixed with second-phase particles. The information extracted from potential CSDs in these systems will contribute to a better understanding of the texture of rocks and may provide a tool to unravel kinetic processes in rocks that contain a coarsening phase and different amounts of second-phase particles.

MODEL

In general, crystalline material will increase in grain size by minimizing surface energy. The kinetics behind this process are dependent on the temperature, time, grain-boundary mobility, and the driving force (given by the volume/surface energy relation; Kretz 1994). The grain boundary mobility depends on the material properties, and also on second-phase particles that are dragged or pinned during grain coarsening (Nes et al. 1985). Therefore, second-phase particles influence the developing mean

crystal size (Zener cited in Smith 1948). The size (d_p) and volume fraction (f_p: dimensionless value between zero and one) of the second-phase particles influence the maximum grain size of the matrix grains, as follows:

$$R = C \frac{d_p}{f_p^m} \tag{3}$$

where C is an empirical constant, and m is an exponent that ranges between 0.33 and 1 (Zener cited in Smith 1948). This Zener relation describes a maximum grain size in a system consisting of a matrix phase and second-phase particles, but it does not provide any CSD due to grain growth. Moreover, according to Zener, the pinning force (F) is given by:

$$F = \frac{3}{2} \gamma \frac{f_p}{d_p} \tag{4}$$

where γ is the grain boundary energy, d_p is the grain size, and f_p is the volume fraction of second-phase particles. This relationship implies that grain growth stops at a limiting diameter:

$$R_L = \frac{3}{2} \frac{f_p}{d_p} \tag{5}$$

These basic relations have been used to develop a grain-growth model for individual neighboring grains (Maazi and Rouag 2002), which can be summarized by:

$$\left(\frac{dR_j}{dt} \right) = 2 M_{ij} A_{ij} \left(\frac{1}{R_j} - \frac{1}{R_i} \pm \frac{3 f_p}{2 d_p} \right) \tag{6}$$

where R_i and R_j are neighboring grains, M is the mobility of the grain boundary between i and j, and A defines the neighborhood relations:

$$Aj = \frac{R_j^2}{\bullet_{j=1}^{N} R_j^2} \tag{7}$$

The role of the Zener pinning effect has a negative (–) sign when $R_i > R_j$ and has a positive (+) sign when $R_i < R_j$. For a detailed discussion of this model, see Maazi and Rouag (2002).

In contrast to the above-mentioned approach, LSW theory does not calculate the processes between individual grains, but uses average critical radii ($R*$ in Eq. 1). In order to develop a geometric model, I will also use average critical radii and replace M and A by an empirical constant as a simplification of the Maazi and Rouag (2002) equations. The main step is to define the minimum (R_{min}) and maximum (R_{max}) critical radii, which are influenced by the d_p/f_p relation (see Eq. 5). The minimum critical radius is given by:

$$R_{min} = \frac{1}{\left(\frac{1}{R*} - \frac{3 f_p}{2 d_p} \right)} \tag{8}$$

In addition, the maximum critical diameter is given by:

$$R_{max} = \frac{1}{\left(\frac{1}{R*} + \frac{3 f_p}{2 d_p} \right)} \tag{9}$$

All initial grains larger than R_{max} will grow and all grains

smaller than R_{min} will shrink. The grains between the minimum and maximum critical parameters do not change their size, because their grain boundaries are fixed by the second phases. Therefore, each grain has three possibilities to change its size, which are defined by the relation between $R*$, R_{min}, and R_{max}. Equation 6 provides a growth relation and kinetics for two grains, which is given by their grain-boundary mobility (Kretz 1994). The grain-boundary mobility at a given temperature is unknown, but can be replaced by an empirical constant K (Eq. 1; see Evans et al. 2001). Using this approach and Equations 6, 8, and 9, we get:

$$\frac{dR}{dt} = \begin{cases} K * \left(\frac{1}{R_{min}} - \frac{1}{R} \right); & R > R_{min} \\ 0 & ; \ R_{max} < R < R_{mi} \\ K * \left(\frac{1}{R_{max}} - \frac{1}{R} \right); & R < R_{max} \end{cases} \quad (10)$$

In this equation, the constant K has a similar physical meaning to K in the LSW equation.

SIMULATIONS OF CSD

Similar to the LSW and CN models, Equations 8–10 can be used to compute CSDs resulting from Zener-influenced coarsening. This iterative type of modeling is limited by the number of grains left in the system after coarsening.

The CSDs can be modeled following the simulation procedure presented in Figure 2. In each cycle, the critical radii ($R_{min, max}$) must be defined. This is important for simultaneous modeling of matrix grain-growth and second phases (e.g., Solomatov et al. 1999). Calculations have been done using the CN equation, the LSW equation, the Zener-influenced Equations 8–10, and the GALOPER program (Eberl et al. 1998, 2000). In CN theory, the harmonic mean of the intercrystal distance is required. This value depends on the population density of the growing phase (see Eq. 2). Following the arguments of Higgins (1998), I combine K and $<1/\lambda>$ into a new constant K'', which is different from the K in the LSW-equation. By using K'' in the CN equation, it is possible

to compare the different kinetic theories (Table 1).

CSD as well as average grain sizes of different models can best be compared at similar amounts of coarsening. Therefore, the amount of coarsening has been defined by:

$$\%\text{growth} = \frac{(R_{mean} - R_{start}) * 100}{R_{start}} \quad (11)$$

where R_{mean} is the average final grain-size and R_{start} is the average grain-size of the starting material. The results of the simulations are presented in Figures 3 and 4, and Tables 1 and 2. I simulated different cycles with constant d_p/f_p values and compare these with other kinetic theories. For completeness, the starting CSD are shown (Fig. 3a). The Zener-influenced model produces asymptotic CSDs, in contrast to the expected Gaussian CSD for LSW calculations (see Fig. 1). The simulated asymptotic CSDs in closed-system coarsening cannot be generated by LSW equations (see also run 4 in Fig. 3). In contrast, CN theory is able to compute trends toward asymptotic CSD, which represent an intermediate shape between the LSW- and the Zener-influenced models (Fig. 3a). The change of the CSD is also documented by plots showing α (natural logarithms of the sizes) vs. β^2 (variance of the natural logarithms) of the computed data (Fig. 3c).

The examples in Figure 3 have one d_p/f_p value (Table 1). In addition, Figure 4 shows the influence of increasing d_p/f_p on the modeled CSDs. It is obvious that high values of d_p/f_p (e.g., low amounts of second-phase particles; Table 1) produce CSDs similar to LSW theory. Because pinning is rare, this result is expected

FIGURE 3. Modeled CSD using different kinetic theories, (**a**) CSD modeled with different equations at similar amount of coarsening (coarsening ~30%): 1 = starting material; Run 2 = the proposed model; Run 4 = LSW model (Eq. 1); Run 6 = CN model (Eq. 2); Run 11 = Ostwald ripening using program-package GALOPER (Eberl et al. 2000). (**b**) An illustration of the effect of high coarsening intensities. Run 3 show the Zener-influenced model at 92% coarsening. (**c**) Calculated statistical parameters for Zener-influenced CSDs plotted in α–β^2 diagram (Eberl et al. 1998). Same input data as in **a** and **b**. Further information on the runs is given in Table 1.
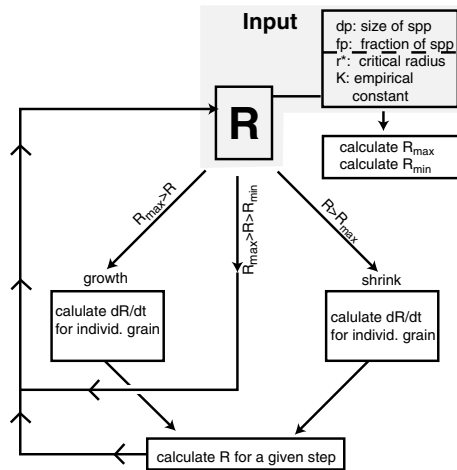
FIGURE 2. Flow diagram showing the simulation procedure. The diagram shows the iteration used for each grain size calculation. The input parameters are shown in the upper right corner.
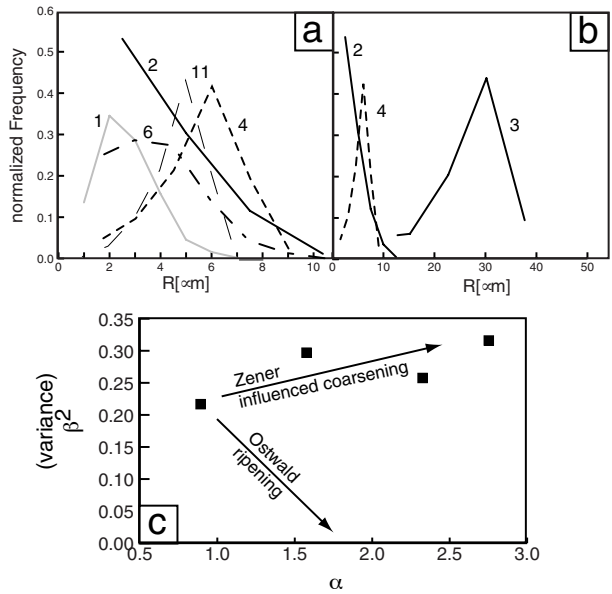
TABLE 1. Data of modeling using LSW-, CN- and Zener-influenced-coarsening (ZIC) equations

Run no.	Model	Cycles no.	K (K″)	f_p	d_p μm	d_p/f_p μm	R* μm	t	Growth %	R_{mean} μm	Grains no.
2	ZIC	1	10	0.1	0.5	5	2	2	39	3.02	618
3	ZIC	2	10	0.1	0.5	5	2	2	92	4.20	569
4	LSW	2	7				2	2	76	3.83	477
5	LSW	2	5				2	2	65	3.6	487
6	CN	1	K″ 3				2	2	37	2.98	625
7	CN	2	K″ 3				2	2	112	4.64	488
8	ZIC	2	10	0.33	0.5	1.5	2	2	13	2.46	691
9	ZIC	2	10	0.01	1	100	2	2	404	10.99	440
10	ZIC	2	10	0.001	2	2000	2	2	432	11.61	430

Notes: Grain size and d_p/f_p ratios are given in micrometers.

TABLE 2. Results from simulations using variable K-values and comparison with LSW-modeling

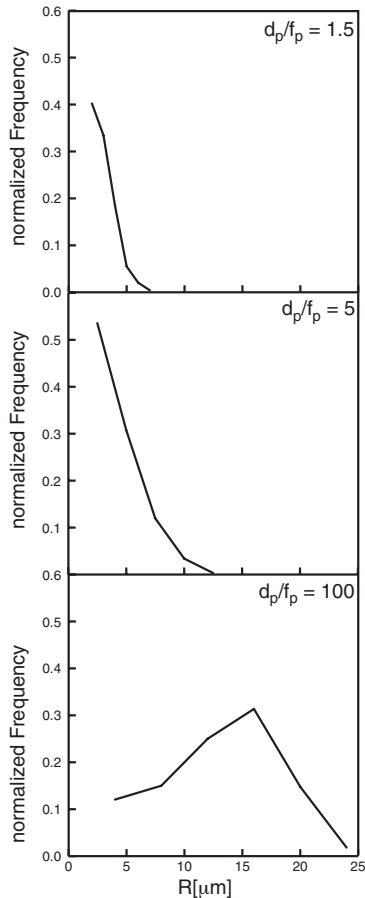| d_p/f_p μm	K	D_{mean} ZIC μm	Growth %	D_{mean} LSW μm	Growth %	Diff in growth %
5	10	3.02	38.52	3.27	50.16	−12
5	10	4.20	92.39	4.80	120.02	−28
5	25	3.89	78.51	4.69	114.86	−36
5	25	7.37	237.78	7.86	260.38	−23
5	100	7.86	260.35	11.50	427.25	−167
5	100	27.21	1147.74	19.30	785.20	363

Notes: For abbreviations see Table 1.

FIGURE 4. Computed CSDs of the Zener-influenced model at variable d_p/f_p ratios. At high d_p/f_p ratios, the CSD shift toward similar shape as LSW or CN modeling (compare also Fig. 3). In contrast, at low d_p/f_p ratios, assymptotic CSD developed which are different from LSW theory. Further information is given in Table 1 (run 8, 9, and 10).

if only a few second-phase particles are present, and the system behaves similar to a pure single-phase systems.

The exact type of CSD depends on the coupled relationship between R* and $R_{min,max}$ (Fig. 5). This relationship changes with variable d_p/f_p. Therefore, the amount and the size of the second-phase particle influences the observed CSD. If d_p/f_p is high, the calculated $R_{min,max}$ is nearly identical for variable R*, and Equation 10 reduces to the LSW grain-coarsening equation. If d_p/f_p is moderate, R_{min} increases exponentially whereas R* and R_{max} increase only slightly (Fig. 5). This exponential increase of the difference between R_{min} and R_{max} produces a stagnation of coarsening. This means that with increasing matrix grain sizes, the available second phases become more and more effective in pinning the moving grain boundaries. An alternative to continued coarsening of the matrix grains at constant f_p is to change d_p as the grain size of the matrix increases. In this case, the discrepancy between R_{min} and R_{max} decreases.

CSD and grain sizes during contemporaneous growth of matrix and second phases can be calculated from the present model by iterative change of d_p (Fig. 2). This calculation is not possible using other kinetic models. The relationship between R* and $R_{min,max}$ indicates the limit of the model. In models with extremely high contents of second-phase particles ($f_p > 0.5$), the relation between R* and R_{min} becomes inconsistent. The definition of matrix grains and second phases becomes ambiguous and grain growth cannot be described by a Zener-influenced coarsening model.

Natural examples

The Adamello pluton produces an approximately 2 km wide contact metamorphic aureole in sedimentary rocks (Brack 1984). One sedimentary unit is the "Calcare di Dosso dei Morti," which represents former stromatoporoid reefs. The contact aureole produced a continuous transition from fine-grained non-metamorphic carbonates to coarse-grained calcite marbles. The grain coarsening during that metamorphism was investigated in the nominally pure marbles (Herwegh and Berger 2003). The non-metamorphic material has an average grain size of 5 μm, whereas the highest-grade rocks consist of centimeter-sized crystals. However, second-phase particles, such as mica, influence the kinetics of coarsening. As a case study, I present results for one sample from the contact aureole, which reached maximum temperatures of ~415 °C. The calcite grain size varies and the sample contains layers with variable amounts of mica (Table 3). The grains were analyzed on images of thin sections. Based on the resulting grain-boundary outlines, the areas of the
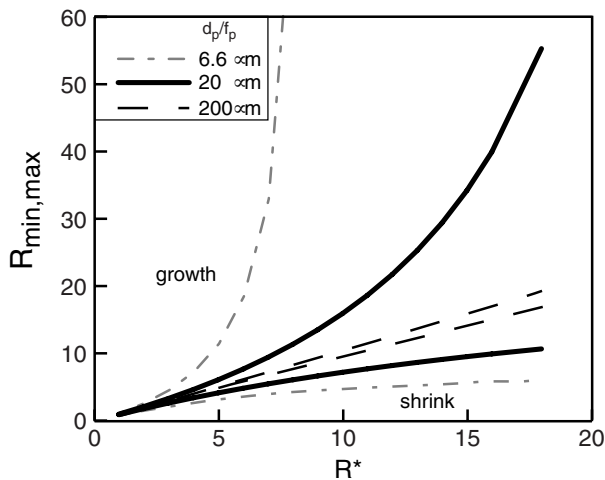
FIGURE 5. Evolution of R_{min} and R_{max} with the critical radius $R*$ and variable d_p/f_p values. In this representation, the effect of different d_p/f_p ratios on the grain size evolution become obvious.

TABLE 3.   Grain size data for Zener influenced marble in the contact aureole from the Adamello pluton

Sample 20-1		Sample 20-2	
Size class	No. crystal	Size class	No. crystal
75	5	50	99
150	51	100	179
225	57	150	86
300	26	200	37
375	18	250	5
450	9	300	3
525	2		
600	2		
D_{mean}	sum	D_{mean}	sum
209	170	88	409
f_p	0.011	f_p	0.068
d_p	25	d_p	28

Notes: Grain size are given in micrometers.

grains were estimated with Image SXM (Version 1.61). The data were checked for 3D-conversion using the computer program "CSDCorrections" (Higgins 2000). The shapes of the CSD in 2D and 3D are similar, which is caused by the isometric shapes and random distributions of the investigated calcite grains. Therefore, a 2D presentation is chosen in order to be comparable with other studies. The calcite grains in the mica-poor sample show a skewed Gaussian distribution, which can be modeled using the LSW equation (Fig. 6a). However, in the mica-bearing layers, the CSD shows a log-normal distribution with a trend to a straight-line pattern (Fig. 6b). This data fit a Zener-influenced CSD (see run 2 in Fig. 3a). The CSD suggests that it developed by closed-system coarsening. The fact that two different CSDs developed during the same temperature-time history in the same rock indicates dependence on d_p/f_p (Fig. 6). Slight changes of the shape of the CSDs are sometimes hard to recognize, but completely different patterns (log-normal vs. asymptotic CSD) clearly can be detected. In addition, statistical parameters (e.g., variance of the distribution; see Fig. 3c) can be used to identify
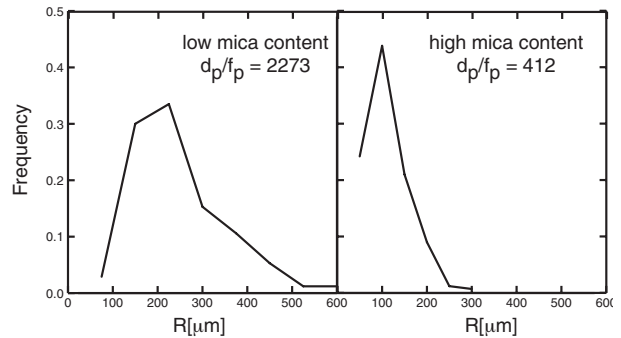

FIGURE 6. CSDs in impure contact-metamorphic marbles. Data are given in Table 3. Note the difference in the CSD pattern for two portions of the same sample at varying mica content. The high mica content produces a log-normal CSD as modeled by the presented model (compare Fig. 3).

the evolution of the distributions. The direct comparison of modeled and measured CSDs enables the use of different models (e.g., Higgins 1998).

The absolute grain size also changes with d_p/f_p in Zener-influenced systems (see Equation 3). Independent of absolute values, the relations between d_p/f_p and grade of coarsening in the model can be compared with natural data. Mas and Crowley (1996) published a data set on calcite coarsening showing variable d_p/f_p. These data show a power-law relationship between d_p/f_p and matrix grain-size (R_{mean}) in the impure rocks. Toward pure carbonates, a break in slope occurs, indicating that grain sizes are not (or only weakly) influenced by second-phase particles. The Zener-influenced coarsening model calculates a change in matrix grain-size with increasing d_p/f_p ratio in the same manner as observed in the natural example by Mas and Crowley (1996; Fig. 7).

The use of zener-influenced coarsening in geological systems

Grain coarsening accompanies increasing intensity of metamorphism. Assuming a stable paragenesis, coarsening will be strongly influenced by the number and distribution of the phases present. Extrapolating experimental data obtained on single-phase systems to regional metamorphic time-temperature scales, much larger grain sizes would be expected. In nature, the grain sizes are strongly influenced by second-phase particles. However, the values of C and m in Equation 3 are not well known. Under these circumstances, the CSD helps to interpret grain-growth processes. Iterative modeling of the CSD gives insights into the extent to which the second-phase particles influence grain growth. This insight is particularly useful where different d_p/f_p values are measured in one locality.

Most metamorphic textures do not suggest pure grain growth, but also include the changes induced in second phases (e.g., abundance and size) by metamorphic reactions. However, in rocks containing one dominant phase, which underwent mainly grain growth, the model is able to include change in size and fraction of the other phases. This situation reflects the case of a variable R_{min} and R_{max} depending on d_p/f_p (see Fig. 5). These changes can be modeled in terms of the CSD and average grain size using the proposed equations.
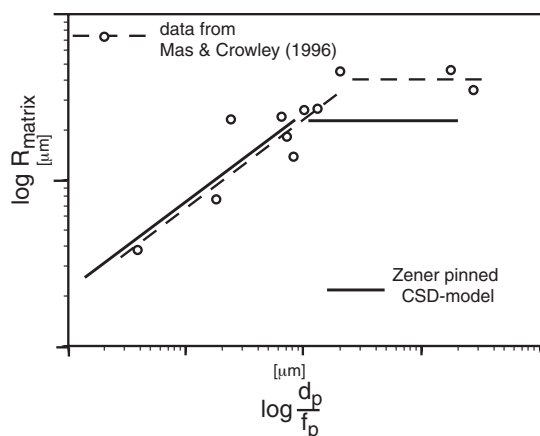
FIGURE 7. Diagram of d_p/f_p vs. matrix grain size. The open circles represent data from Mas and Crowley (1996) and the dashed line is a fit through this data. The solid line was calculated using the present coarsening model. The model is reduced to the average grain size, but the dependency of d_p/f_p on the matrix grain size can be simulated.

CONCLUDING REMARKS

The model presented here calculates grain-size limits based on the relation of volume-fraction and size of second-phase particles. The resulting CSDs differ from those of LSW-based CSDs in the case of closed-system coarsening. This difference is caused by the ability of the model to fix some grain sizes by pinning due to the presence of second phases. The developed grain sizes depend on d_p as well as on f_p.

This model has great potential for comparing calculated and measured CSDs in metamorphic rocks. In samples with measurable CSD, d_p, and f_p (e.g., Mas and Crowley 1996), the CSD can be modeled for grain-size evolution along a given temperature-time path. In these examples, the measured average grain size as well as the parameters of the CSD can be compared with calculated ones. If it is possible to quantify the effect of second-phase particles, we can also adapt experimental data for single-phase grain growth to a wider range of natural examples.

REFERENCES CITED

Brack, P. (1984) Multiple Intrusion—Examples from the Adamello Batholith and their signifcance of the mechanism of intrusion. Memoire della Societa Geologica Italia, 26, 145–157.
Brook, R.J. (1976) Controlled grain growth. In F.Y. Wang, Ed., Ceramic fabrication processes (treatise on material science and technology), 9, p. 331–364. Academic Press, New York.
Cabane, H., Laporte, D., and Provost, A. (2001) Experimental investigation of the kinetics of Ostwald ripening of quartz in silicic melts. Contributions of Mineralogy and Petrology, 142, 361–373.
Cashman, K.V. and Marsh, B.D. (1988) Crystal size distrubution (CSD) in rocks and kinetics and dynamics of crystallization. 2. Makaopuhi lava lake. Contribution

of Mineralogy and Petrology, 99, 292–305.
Chai, B.H.T. (1974) Mass transfer of calcite during hydrothermal recrystallization. In Hofmann, A.W., Giletti, B.J., Yoder, H.S.J., and Yund, R.A., Eds., Geochemical transport and kinetics, 634, p. 205–218. Carnegie Institut of Washington.
Covey-Crump, S.J. (1997) The normal grain growth behavior of nominally pure calcitic aggregates. Contributions to Mineralogy and Petrology, 129, 239–254.
Covey-Crump, S.J. and Rutter, E.H. (1989) Thermally induced grain growth of calcite marbles on Naxos Island, Greece. Contributions to Mineralogy and Petrology, 101, 69–86.
DeHoff, R.T. (1991) A geometrically general theory of diffusion controlled coarsening. Acta Metallica Materiala, 39, 2349–2360.
Denison, C. and Carlson, D. (1997) Three dimensional quantitative textural analysis of metamorphic rocks using high resolution computed X-ray tomography: Part II. Application to natural samples. Journal of Metamorphic Geology, 15, 45–57.
Eberl, D.D., Drits, V.A., and Środoń, J. (1998) Deducing growth mechanisms for minerals from the shapes of crystal size distributions. American Journal of Science, 298(6), 499–533.
——— (2000) User's Guide to GALOPER-A program for simulating the shapes of crystal size distributions-and associated Programs. U.S. Geological Survey Open File Report, OF 00-505, 44 p.
Eberl, D.D., Kile, D.E., and Drits, V.A. (2002) On geological interpretations of crystal size distributions: Constant vs. proportionate growth. American Mineralogist, 87, 1235–1241.
Evans, B., Renner, J., and Hirth, G. (2001) A few remarks on the kinetics of static grain growth in rocks. International Journal of Earth Science, 90, 88–103.
Herwegh, M. and Berger, A. (2003) Changes in calcite growth behavior: Field data-based modeling of grain growth. Contributions of Mineralogy and Petrology, 145, 600–611.
Higgins, M.D. (1998) Origin of anorthosite by textural coarsening: Quantitative measurements of a natural sequence of textural development. Journal of Petrology, 39, 1307–1323.
———(2000) Measurement of crystal size distribution. American Mineralogist, 85, 1105–1116.
———(2002) A crystal size distribution study of the Kiglapait layered mafic intrusion, Labrador, Canada: evidence for textural coarsening. Contributions of Mineralogy and Petrology, 144, 314–330.
Joesten, R.L. (1991) Kinetics of coarsening and diffusion controlled mineral growth. In Derrill M. Kerrick, Ed., Contact metamorphism, 26, 507–582. Reviews in Mineralogy, Mineralogical Society of America, Washington, D.C.
Kretz, R. (1994) Metamorphic crystallization, 507 p. Wiley, New York.
Lifshitz, I.M. and Slyozov, V.V. (1961) The kinetics of precipitation from supersaturated solid solutions. Journal of Physics and Chemistry of Solids, 19, 35–50.
Maazi, N. and Rouag, N. (2002) Consideration of Zener drag effect by introducing a limiting radius for neighbourhood in grain growth simulations. Journal of Crystal Growth, 243, 361–369.
Marsh, B.D. (1988) Crystal Size distribution (CSD) in rocks and kinetics and dynamics of crystallization. 1. Theory. Contribution of Mineralogy and Petrology, 99, 277–291.
———(1998) On the interpretation of crystal size distributions in magmatic systems. Journal of Petrology, 39, 553–599.
Mas, D.L. and Crowley, P.D. (1996) The effect of second phase particles on stable grain size in regionally metamorphosed polyphase calcite marbles. Journal of Metamorphic Geology, 14, 155–162.
Masuda, T., Morikawa, T., and Nakayama, Y. (1997) Grain-boundary migration of quartz during annealing experiments at high temperatures and pressures, with implications for metamorphic geology. Journal of Metamorphic Geology, 15, 311–322.
Nes, E., Ryum, N., and Hunderi, O. (1985) On the Zener drag. Acta Metallurgica, 33, 11–22.
Nichols, S.J. and Mackwell, S.I. (1991) Grain-growth in porous olivine aggregates. Physics and Chemistry of Minerals, 18, 269–278.
Solomatov, V.S., El-Khozondar, R., and Tikare, V. (2002) Grain size in the lower mantle: constraints from numerical modeling of grain growth in two-phase systems. Physics of the Earth and Planetary Interiors, 129, 265–283.
Smith, C.S. (1948) Grains, phases, and interphases: An interpretation of microstructure. Transaction of the American Institut Mineralic and Metallic Engineering, 175, 15–51.
Wagner, C. (1961) Theorie der Alterung von Niederschlägen durch Umlösen (Ostwald Reifung). Zeitschrift Elektrochemie, 65, 581–591.